Fig 1

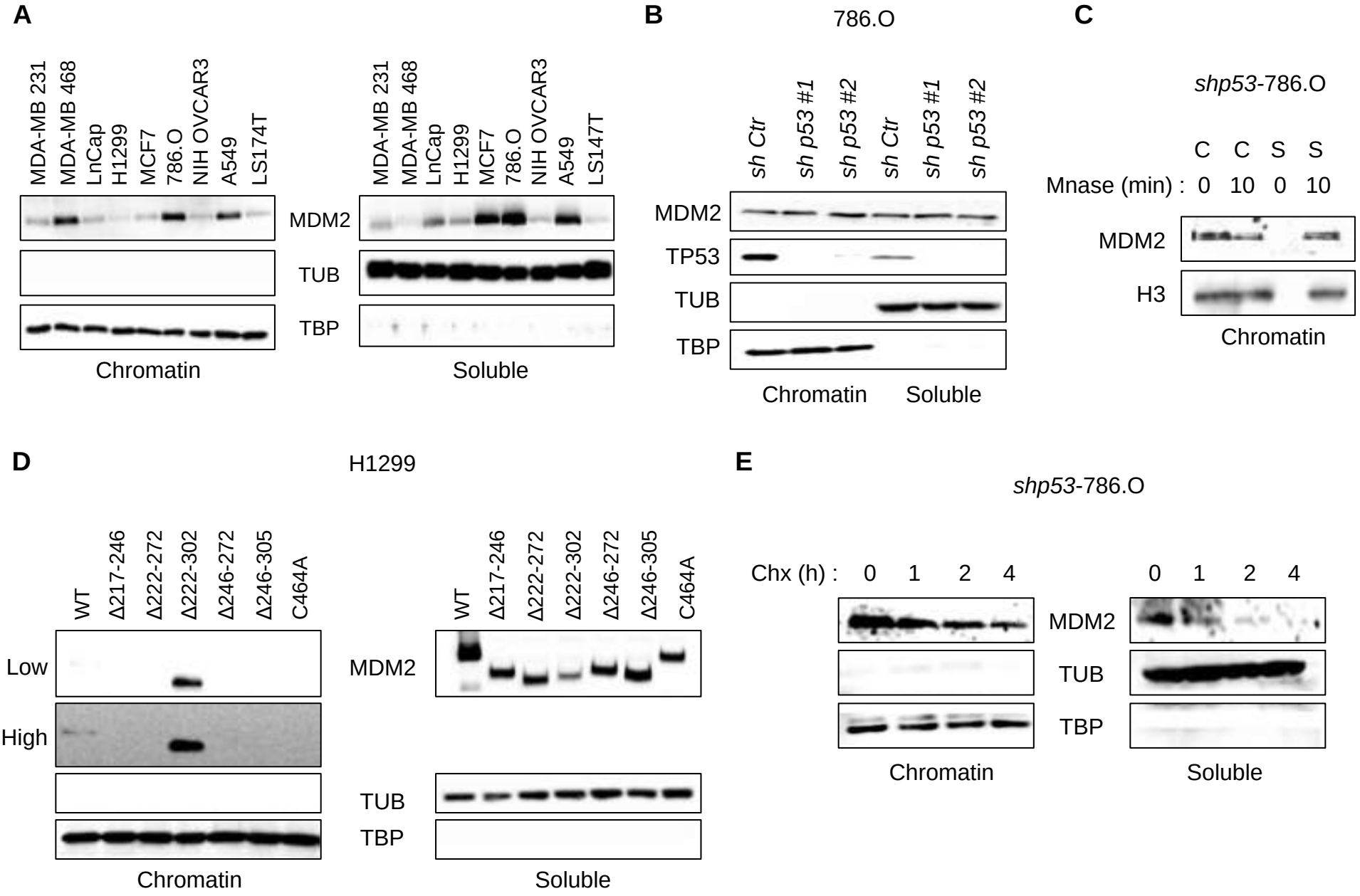
A
MDA-MB 231
MDA-MB 468
LnCap
H1299
MCF7
786.O
NIH OVCAR3
A549
LS174T
MDM2
TUB
TBP
Chromatin
Soluble
B
786.O
sh Ctr
sh p53 #1
sh p53 #2
sh Ctr
sh p53 #1
sh p53 #2
MDM2
TP53
TUB
TBP
Chromatin
Soluble
C
shp53-786.O
C C S S
Mnase (min) : 0 10 0 10
MDM2
H3
Chromatin
D
H1299
WT
Δ217-246
Δ222-272
Δ222-302
Δ246-272
Δ246-305
C464A
Low
High
MDM2
TUB
TBP
Chromatin
Soluble
E
shp53-786.O
Chx (h) : 0 1 2 4
0 1 2 4
MDM2
TUB
TBP
Chromatin
Soluble

Fig 2

A

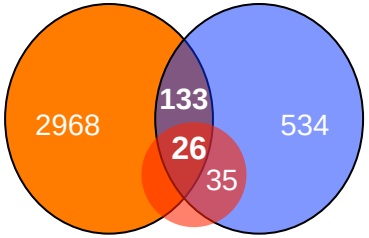

B

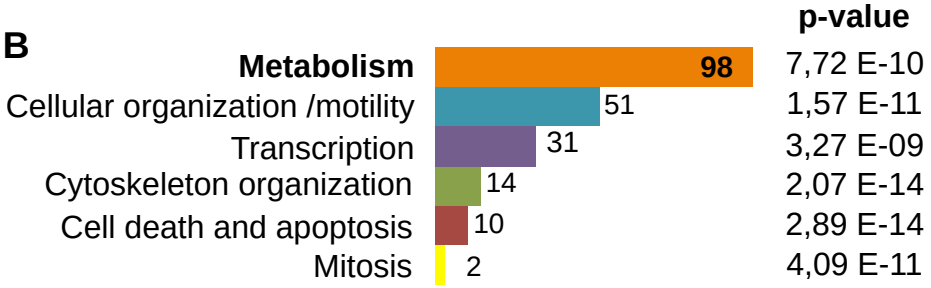

C

Co-cited TFs	P-value	Genes (observed)	Genes (expected)
ATF3	**1,23E-07**	**14**	**2,79**
ATF4	**1,96E-07**	**12**	**1,76**
HSF1	2,11E-05	9	1,51
TFAP4	7,99E-05	6	0,71
MAX	2,77E-04	5	0,57
FOXQ1	6,34E-04	6	1,04
MXD1	6,94E-04	4	0,40
ASXL3	8,22E-04	2	0,04
ZFHX4	8,92E-04	3	0,19
RARA	1,17E-03	8	2,08

26 ATFs target genes

ABL1
ANKRD1
ANXA1
ASNS
BDNF
CDH4
CEBPB
CENPE
CHAC1
CLDN1
DKK1
DUSP5
EMP1
HSP90AA1
PCK2
PHLDA1
PIK3R3
PSAT1
SCG5
SERPINC1
SLC1A4
SLC7A11
SLC7A5
SLC38A2
YWHAE
ZFHX3

D

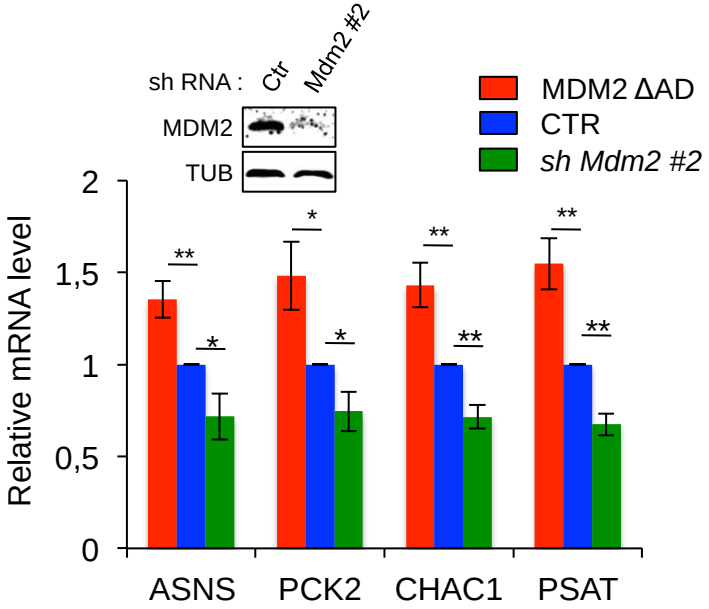

E

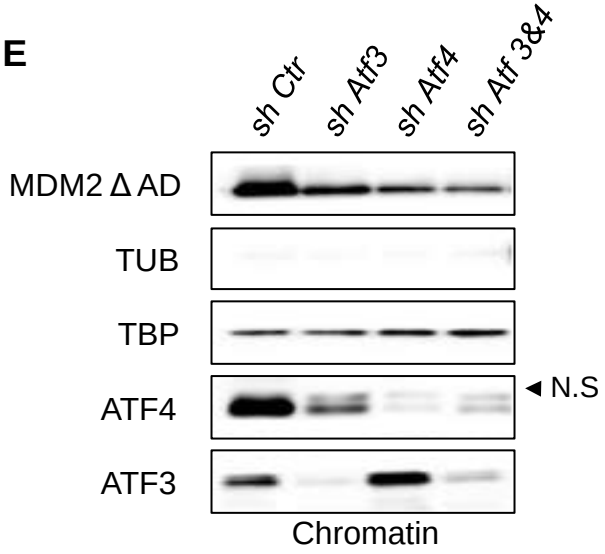

F

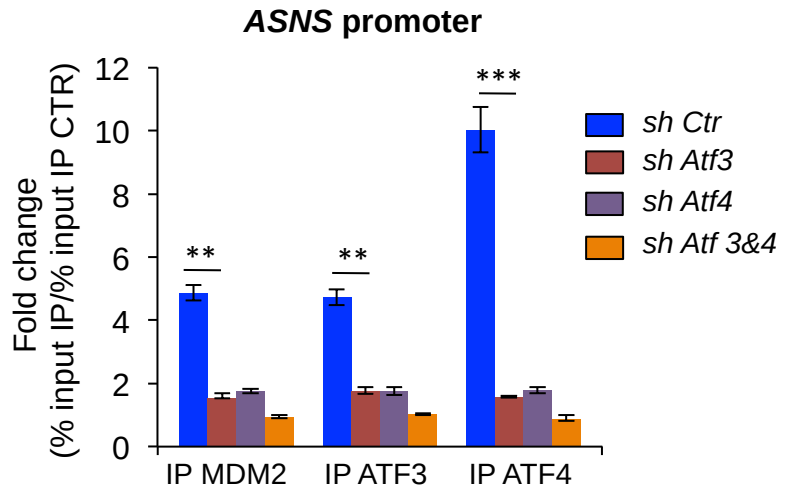

Fig 3

A

Pathways	Metabolism	Transport
Serine / Glycine pathway	*CBS, CTH, PSAT1, PSPH, PHGDH, SHMT2, ALDH1L2,GART,GOT1,GPT2, MTHFD1L, MTHFD2*	*SLC1A4, SERINC1*
Glutamine/ Glutamate pathway	*GOT1, GPT2, ASNS, BCAT1, SIRT4*	*SLC38A2, SLC38A1, SLC7A11, SLC7A7*
Cysteine/Cystine pathway	*CBS, CTH, ETHE1*	*SLC7A11, SLC7A9, SLC1A4*
Other amino acid pathway	*ADC, AMDHD1, ANXA1, ARG2, BDNF, CARS, CHAC1, CTNS, GARS,GGACT, GGTLC1, GPX1, HBB, IARS, LARS, MARS, MSRA, NEDD4L, NQO1,PSEN1, PSMB6, PYCR1, SARS, TARS, TNF, VNN1, WWP2, YWHAE*	*AQP1,KCNE1L, KCNMA1, KCNT2, PDZK1, SLC25A16, SLC25A20, SLC38A8, SLC3A2,SLC43A2, SLC7A5, SLCO1B1, SLCO1B3, SYT1,SLC7A1, SLC6A15*

B

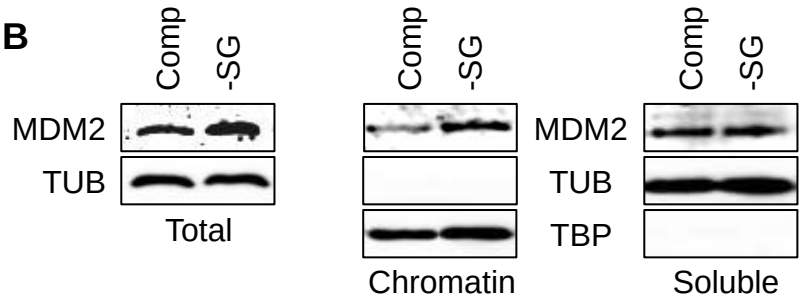

C

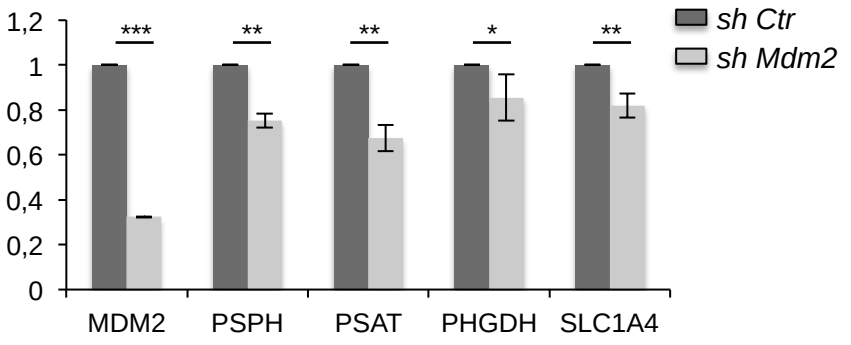

D

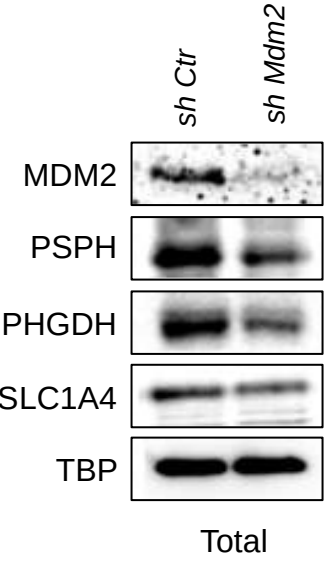

E

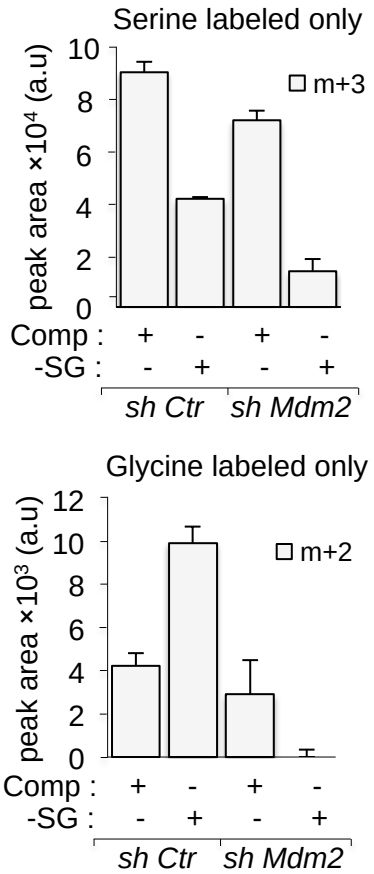

F

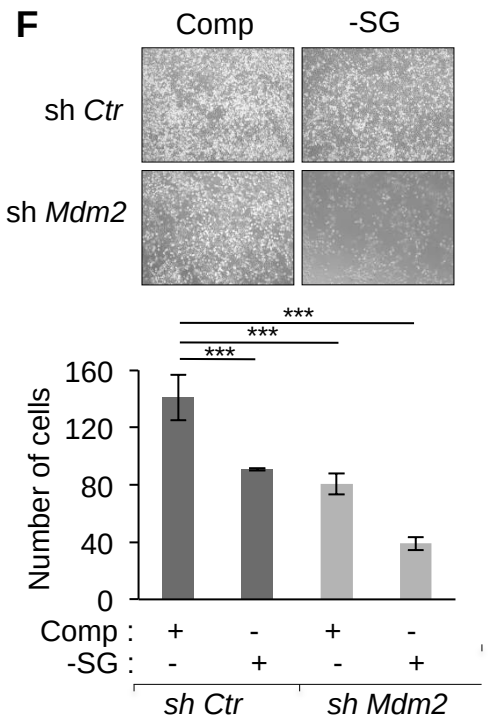

G

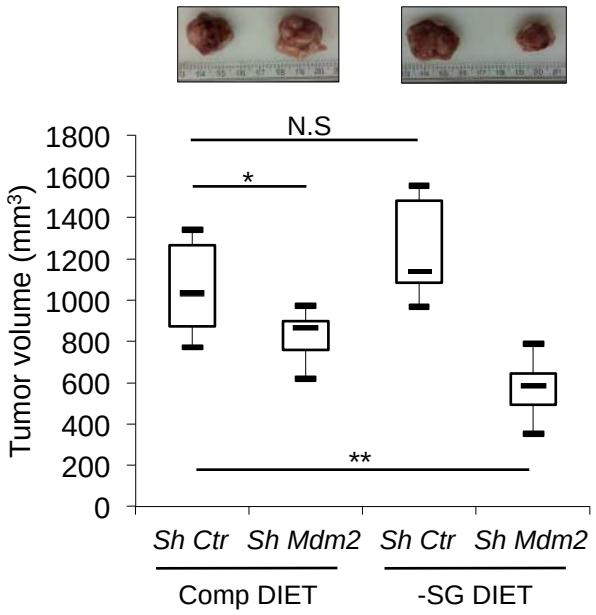

Fig 4

A

glutathione synthesis	*ACOT12,CBS, CTH, CTNS, EHHADH, ETHE1, HS2ST1, NPAS2, PHGDH, SHMT2, TXNRD3*
glutathione recycling	*GPX1, GSTT2, GCACT, GGTLC1*
other response to oxidative stress	*NQO1, MSRA, VNN1, PYCR1*

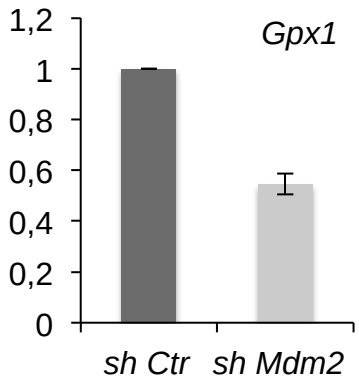

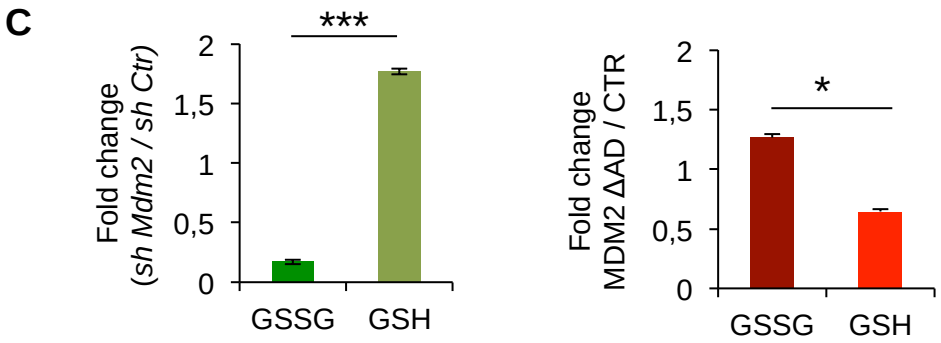

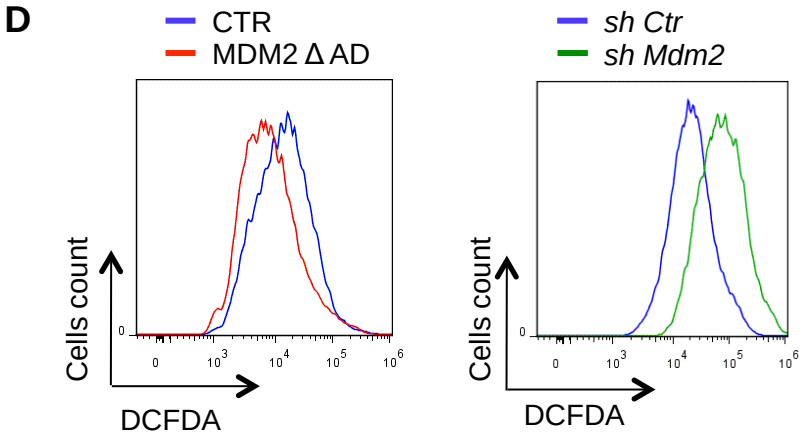

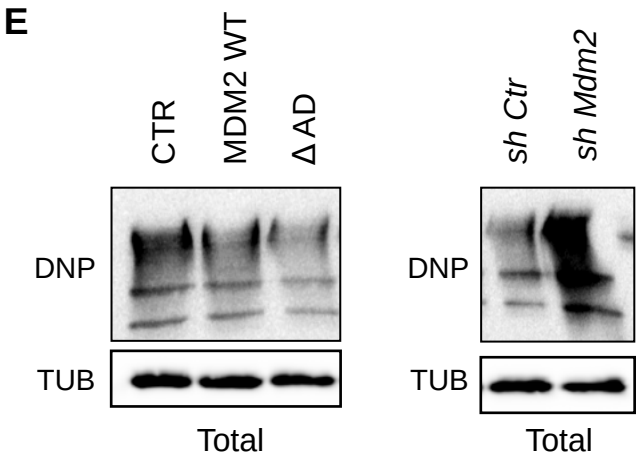

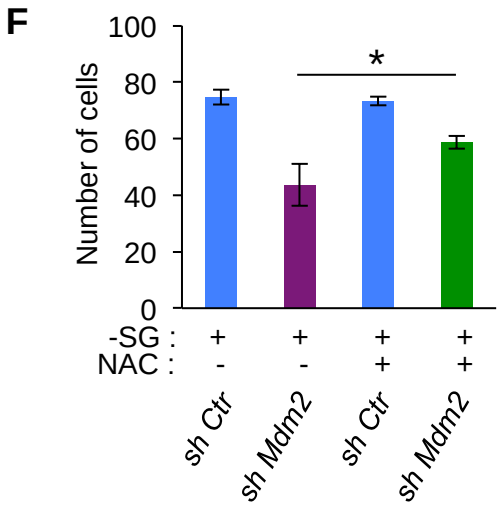

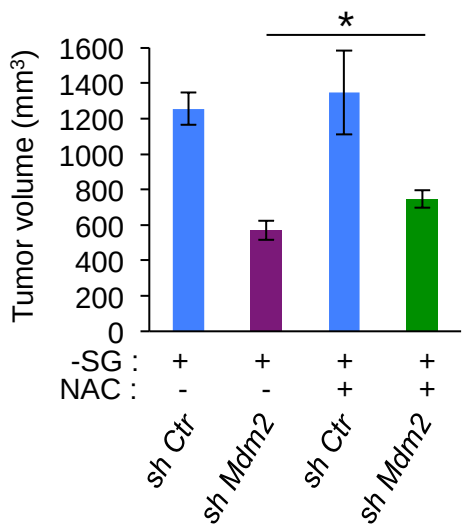

Fig 5

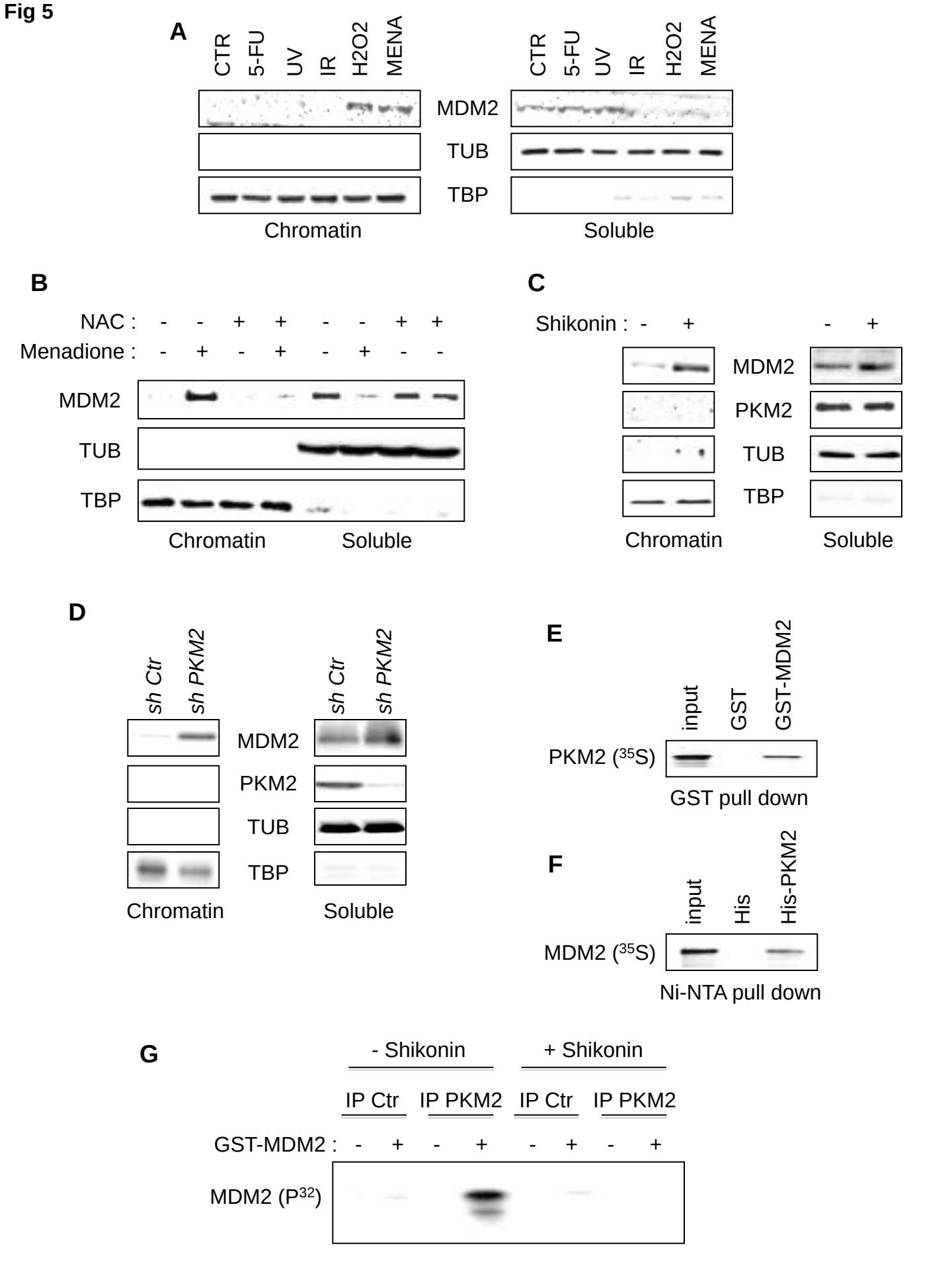
A
CTR
5-FU
UV
IR
H2O2
MENA
MDM2
TUB
TBP
Chromatin
Soluble
B
NAC :
Menadione :
MDM2
TUB
TBP
Chromatin
Soluble
C
Shikonin :
MDM2
PKM2
TUB
TBP
Chromatin
Soluble
D
sh Ctr
sh PKM2
MDM2
PKM2
TUB
TBP
Chromatin
Soluble
E
input
GST
GST-MDM2
PKM2 (35S)
GST pull down
F
input
His
His-PKM2
MDM2 (35S)
Ni-NTA pull down
G
- Shikonin
+ Shikonin
IP Ctr
IP PKM2
IP Ctr
IP PKM2
GST-MDM2 :
MDM2 (P32)

Fig 6

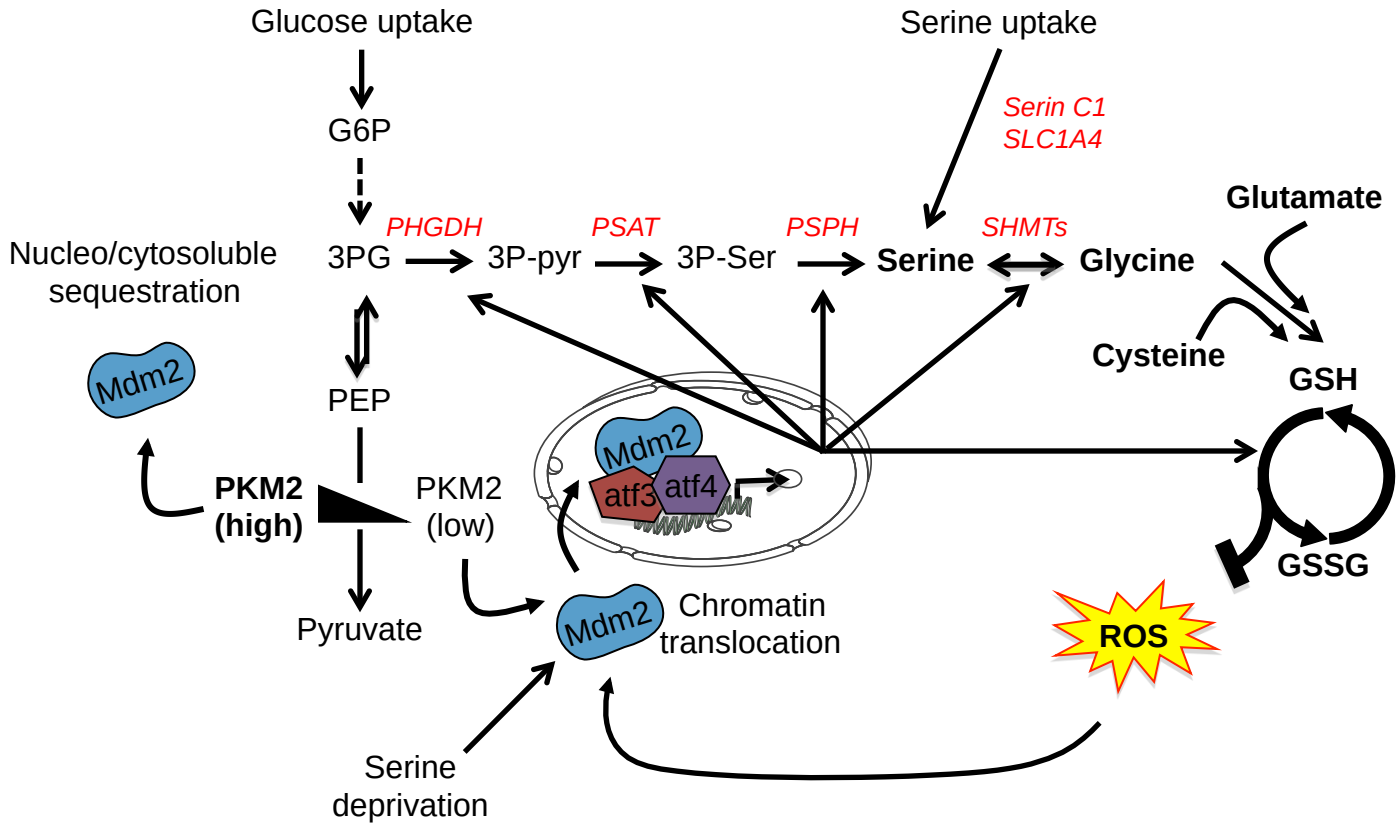
Glucose uptake
G6P
Serine uptake
Serin C1
SLC1A4
PHGDH
PSAT
PSPH
SHMTs
Glutamate
Nucleo/cytosoluble
sequestration
3PG
3P-pyr
3P-Ser
Serine
Glycine
Cysteine
GSH
GSSG
Mdm2
PEP
Mdm2
atf3
atf4
PKM2
(high)
PKM2
(low)
Pyruvate
Mdm2
Chromatin
translocation
ROS
Serine
deprivation

Figure legends

Figure 1: Mdm2 is localized in chromatin independently of p53

(A) MDM2 localization in different cancer cell lines after biochemical fractionation. Fractions enriched in chromatin-associated proteins (chromatin) were separated from pooled fractions containing nucleo- and cyto- soluble proteins (soluble) and analyzed by immunoblotting for the indicated proteins. The quality of the fractionation and equal loading was verified by Tata Binding Protein (TBP) and Tubulin (TUB) expression. (B) Immunoblot analyses of the indicated proteins in 786.O cells expressing a control- or p53- shRNAs after biochemical fractionation. (C) Chromatin-bound MDM2 was solubilized after digestion of DNA of the chromatin fraction (C) by Micrococcal nuclease (Mnase, 10 min) and recovered in the supernatant (S). Release of Histone H3 from chromatin was used as a control of Mnase efficiency. (D) Localization of the indicated MDM2 mutants after ectopic expression in H1299 cells. Low and high exposure of the MDM2 immunoblot are shown. (E) Half life of endogenous chromatin-bound or soluble MDM2 in p53-shRNA treated 786.O cells after incubation with cycloheximide (CHX) for the indicated time. In all panels, protein expression of MDM2, TUB, H3, TBP and p53 was measured by quantitative immunoblotting.

Figure 2: Chromatin bound MDM2 regulates an ATF-dependent transcriptional program

(A) Venn diagram illustrating the number of MDM2 target genes identified by MDM2 ChIP-sequencing and expression profiling of p53 null H1299 cells expressing the MDM2ΔAD (Δ222-302) mutant. MDM2 binding sites were identified by ChIP-seq

performed in H1299 cells using MACS with a *p* value = 5.10^{-5} by subtracting peaks identified in *Mdm2* shRNA treated cells to those identified in control shRNA treated cells and cells expressing the MDM2ΔAD mutant. This gene list was intersected with the list of transcripts identified by microarray that showed differential expression between cells transfected with MDM2-ΔAD mutant and control cells transfected with the empty vector (*p* value ≤0.001). The number of ATF target genes in this gene list is indicated in red in the Venn diagram. (B) Functional annotation of this restricted list of 159 MDM2 direct target genes identified by these combined pan-genome approaches in H1299 cells. (C) Gene to transcription factor associations within MDM2 target genes using data mining algorithms (genomatix) showing significant enrichment in ATF3/4 target genes. (D) Relative mRNA level of a representative panel of ATF target genes in MDM2-depleted H1299 cells (sh*Mdm2*) or in cells expressing the MDM2ΔAD mutant. Data were determined by RT-qPCR and normalized to the corresponding control samples prepared from H1299 cells transfected with an empty vector or expressing a control shRNA (mean +/- SD; n=8). The inset shows the protein level of MDM2 in H1299 cells expressing control- or Mdm2- shRNA. (E) Immunoblot analyses showing the level of chromatin associated MDM2ΔAD in H1299 cells expressing shRNAs targeting *Atf3* and/or *Atf4* after subcellular fractionation (ns, non specific band). (F) Quantitative chromatin immunoprecipitation (qChIP) experiments showing the relative recruitment of MDM2, ATF3 and ATF4 on the *Asns* locus in H1299 expressing control-, *Atf3*- and/or *Atf4*-shRNAs, as indicated. Results were represented as the relative ratio between the mean value of immunoprecipitated chromatin (calculated as a percentage of the input) with the

indicated antibodies and the one obtained with a control irrelevant antibody (mean ± SEM; n=3 independent experiments).

*$p \leq 0.05$, **$p \leq 0.01$ and *** $p \leq 0.001$ indicate statistical significance of the observed differences.

Figure 3: Serine/glycine deprivation regulates MDM2 recruitment to chromatin

(A) Gene set enrichment analysis (GSEA) of MDM2 responsive genes determined by gene expression profiling of H1299 cells expressing the MDM2ΔAD mutant (*p* value ≤0.005). Subclasses within the amino acid transport and metabolism category highlighted serine/glycine, glutamine/glutamate and cysteine metabolism. (B) Serine/glycine deprivation increases MDM2 recruitment to chromatin. Immunoblot analysis of MDM2 protein level in whole cell extracts (Total), or in fractions enriched in chromatin-associated (chromatin) or nucleo- and cyto- soluble (soluble) proteins prepared from H1299 cells cultured in complete medium (Comp) or in the same medium lacking serine and glycine (-SG). The quality of the fractionation and equal loading was verified by Tata Binding Protein (TBP) and Tubulin (TUB) expression. (C) Relative mRNA level of the MDM2-target genes *Psph*, *Psat*, *Phgdh*, and *Slc1A4* in H1299 cells expressing a control- or *Mdm2*- shRNA cultured in complete medium for 48 hours. Data were determined by RT-qPCR (mean +/- SD; n=5). (D) Immunoblot analysis of PSPH, PHGDH and SLC1A4 protein levels in total cell extracts prepared from H1299 cells expressing a control- or *Mdm2*- shRNA cultured in complete medium for 48 hours. (E) Stable isotope tracing experiments. H1299 cells expressing a control- or *Mdm2*- shRNA were cultured in complete (Comp) or serine/glycine-deprived (-SG) medium for 24 h, in the presence of uniformly labelled [U-^{13}C]glucose for the final hour. LC–MS was used to

detect relative intracellular quantities of ^{13}C-labelled (m+3) serine (upper panel) or (m+2) glycine (lower panel). Histobars represent the mean value of the peak area +/- SD (arbitrary unit) corresponding to serine and glycine peaks on the MS-chromatogram. The experiment was performed in triplicate. (F) Microphotograph of control- or *Mdm2*-shRNA treated H1299 cells cultured for 4 days in complete medium (Comp) changed every 24h or in serine/glycine-deprived (-SG) medium, as indicated. Histobars represent the relative number of cells in those conditions (mean +/- SD; n=3 independent experiments performed in triplicates). (G) Nude mice were subcutaneously xenografted with H1299 cells stably expressing a control- or *Mdm2*- shRNA, and fed with a complete or a serine and glycine deprived diet, as indicated. Box and whisker plots represent the tumor volume (mean +/- SD, n=7 tumors per group) in each experimental group measured when the first animal reached the ethical end-point. Microphotograph of a representative tumor for each experimental group is shown.

*$p \leq 0.05$, **$p \leq 0.01$ and *** $p \leq 0.001$ indicate statistical significance of the observed differences. NS: not significant

Figure 4: MDM2 regulates ROS homeostasis in H1299 cells

(A) Gene list of MDM2 target genes implicated in glutathione metabolism determined by gene expression profiling of H1299 cells expressing the MDM2ΔAD mutant (*p* value ≤0.005). (B) RT-qPCR analysis of *Gpx1* mRNA level in H1299 cells expressing a control or *Mdm2* shRNA cultured in complete medium. The histobars represent the mean value +/- SD of n=3 independent experiments. (C) Determination of the relative level of oxidized (GSSG) and reduced (GSH) glutathione in H1299 cells expressing a control- or

Mdm2- shRNA (left panel), or in H1299 cells transfected with an empty vector or expressing the MDM2ΔAD mutant (right panel) (mean +/- SD, n=3). (D-E) MDM2 controls the redox state of cancer cells independently of p53. (D) Left panel: ROS levels were determined in H1299 cells transfected with an empty vector or with the MDM2ΔAD mutant by flow cytometry using the redox-dependent fluorophore dichlorodihydrofluorescein diacetate (DCFDA) probe. Right panel: similar experiments were performed in H1299 cells expressing control- or *Mdm2*- shRNA. Data are representative of 4 independent experiments. (E) Immunoblot analyses of the level of protein carbonylation (DNP) in control H1299 cells or cells expressing ectopic WT MDM2 or the MDM2ΔAD mutant (left panel), or in H1299 cells expressing control- or *Mdm2*- shRNA (right panel). (F) The ROS scavenger N-acetyl-cysteine (NAC) partly rescues the growth of MDM2-deficient H1299 cells cultured in serine/glycine deprived medium (-SG). Histobars represent the relative number of cells in the indicated conditions (mean +/- SD; n=3 independent experiments performed in triplicates). (G) NAC treatment partly rescues tumor growth of MDM2-deficient H1299 cells in nude mice. Tumor volume (mean +/- SD, n=7 tumors per group) in each experimental group measured when the first animal reached the ethical end-point.

*P ≤ 0.05 indicate statistical significance of the observed differences.

Figure 5: ***PKM2 and oxidative stress control MDM2 recruitment to chromatin***

(A) MDM2 localization in H1299 cells was determined by immunoblotting in chromatin and soluble fractions prepared after DNA damage (5-fluorouracil (5FU), UV, or ionizing

radiation (IR)) or after treatment with pro-oxidants (H2O2, Menadione (MENA)). The quality of the fractionation and equal loading was verified by Tata Binding Protein (TBP) and Tubulin (TUB) expression. (B) MDM2 localization in H1299 cells upon menadione-induced oxidative stress in presence or absence of the ROS-scavenger N-acetyl-cysteine (NAC). (C, D) PKM2 activity influences MDM2 recruitment to chromatin. The level of chromatin-bound MDM2 was evaluated by immunoblotting in mock-treated H1299 cells or in cells treated with the pharmacological PKM2 inhibitor shikonin (C) or in cells expressing *Pkm2* shRNA (D). (E) GST-pull down assays performed with in vitro translated (IVT) [^{35}S]-methionine radiolabelled PKM2 and GST or GST-MDM2. (F) Affinity purification on Nickel-NTA columns of IVT [^{35}S]-methionine radiolabelled MDM2 with bacterially produced recombinant histidine-tagged PKM2 (HIS-PKM2). (G) In vitro kinase assays performed with endogenous PKM2 immunoprecipitated (IP) from H1299 cells and purified recombinant GST-MDM2 protein as a substrate in presence of [^{32}P]-ATP. PKM2 was immunoprecipitated from mock or shikonin-treated H1299 cells, as indicated.

Figure 6: MDM2 is a key regulator of metabolism to sustain cellular anti-oxidant defenses. Model showing how the recruitment of MDM2 to chromatin contributes to serine/glycine and glutathione metabolism. MDM2 recruitment to ATF3/4-target genes is increased upon serine deprivation, oxidative stress or low PKM2 activity to sustain the expression of genes involved in serine/glycine metabolism and in the glutathione cycle. G6P: glucose 6-phosphate; PEP: phosphoenolpyruvate; 3PG: 3-phosphoglycerate; 3P-Pyr: 3-phosphohydroxypyruvate; 3P-Ser: 3-phosphoserine.